Jalalvand, M., Wisnom, M. R., Hosseini-Toudeshky, H., & Mohammadi, B. (2014). Experimental and numerical study of oblique transverse cracking in cross-ply laminates under tension. Composites Part A: Applied Science and Manufacturing, 67, 140-148. 10.1016/j.compositesa.2014.08.004

Experimental and numerical study of oblique transverse cracking in cross-ply laminates under tension

Meisam Jalalvand[a,1], Michael R. Wisnom[a], Hossein Hosseini-Toudeshky[b], Bijan Mohammadi[c]

[a] Advanced Composites Centre for Innovation and Science, University of Bristol, UK

[b] Department of Aerospace Engineering, Amirkabir University of Technology, Tehran, Iran

[c] School of Mechanical Engineering, Iran University of Science & Technology, Tehran, Iran

Abstract

The first damage mode in cross-ply laminates under tension is broadly accepted as transverse cracks normal to the loading direction in the 90° layers, but there is not the same agreement about the second damage mode. While most of the analytical and experimental results are based on delamination induced by transverse cracking, another type of damage, oblique cracks within the 90° layers, has also been observed as the second damage mode in $[0/90_4]_s$ laminates. To understand the cause of this phenomenon, FE analyses considering damage development at the interfaces were performed. The obtained results indicate that the main reason for the oblique cracking damage mode is the higher toughness of the material in mode-II compared with mode-I: when the value of shear toughness is close to the opening toughness, the second damage mode in cross-ply laminates under tensile loading is delamination induced by transverse cracks, however, if the difference between the two values is large, oblique cracks in the 90° layers are likely to appear. In the specific tested and analysed laminate, if the mode II toughness is double the mode I toughness, oblique cracking occurs but if the values of mode I and mode II toughness are close, delamination is the second damage mode.

[1] Corresponding author – M.Jalalvand@Bristol.ac.uk
Composites Part A: Applied Science and Manufacturing Vol 67, Page: 140-148

Keywords:

A) Carbon fibres. B) Delamination. C) Finite element analysis (FEA). C) Transverse cracking. D) Optical microscopy

1. Introduction

The damage process of cross-ply laminates has been widely investigated over many years with a variety of approaches. The first damage mode is broadly accepted as transverse cracking based on different experimental observations [1-4] and theoretical analyses [5-14]. But the observed and predicted second damage mode in cross ply laminates can be categorised in two groups. Most of the observations and analyses have shown that delamination initiating from the tips of the transverse cracks is the second damage mode after the 90° layers reach saturation with transverse cracks [3, 5, 15, 16]. On the other hand, oblique and curved transverse cracks close to the straight ones with no delamination have been also reported as the second damage mode in cross-ply laminates in a few observations [16-18]. These damage modes are shown schematically in Figure 1. There are reports [13, 18] showing these two different kind of secondary damage modes in the same $[0/90_4]_s$ layups when the materials were different.

The occurrence of delamination induced by transverse cracks is mostly described by the stress concentration around the transverse crack tip and also the high value of strain energy release rate. Further transverse cracking and delamination initiating from the tips of existing transverse cracks are known as two competing damage mechanisms. To find the winning mechanism, the energy release rate for transverse cracking and delamination induced by transverse cracks are compared. Different mathematical approaches such as variational [7, 12], shear-lag [3, 6] and Finite Element Analysis (FEA) [19, 20] have been introduced for calculating the energy release rates, all of which may be used in comparing the energy release rates to predict the dominant damage mode. Recently, there have been some studies modelling a longer part of the cross-ply laminate considering the randomness of transverse cracking [21, 22], without the assumption

of uniform transverse crack density. However, the presumed damage mechanisms in all of these analyses are confined to straight transverse cracks covering the whole thickness of the 90° layers and interlaminar cracks at the 0°/90° interface initiating from the tips of transverse cracks.

Tiny oblique cracks in the 90° layers is another damage mode reported to occur after straight transverse cracks. To the best knowledge of the authors, this kind of damage mode has not been investigated in detail and the few available descriptions such as by Groves et. al.[18] and Hu et. al. [16] are not in agreement with each other. Hu et. al. used a variational approach to find the distribution of maximum principal stress around the normal crack tips and showed that at high crack densities, the point with maximum first principal stress moves significantly away from the tips of the straight transverse cracks. However, the stress distribution obtained by Groves et.al. using FEA clearly indicated that the maximum first principal stress stays at or very close to the tips of the straight transverse cracks if linear elastic material properties are applied. They proposed that taking the nonlinearity of the material response into account may improve the agreement between the obtained results and the experimental observations.

In this study, 14 tensile specimens of a cross-ply laminate have been used to assess the damage initiation and propagation at different stages of loading. Similar to all other works, the first observed damage mode was transverse cracking normal to the loading direction but the second observed damage mode was oblique cracking. No delamination was observed. The occurrence of this damage mode is then investigated using FE analyses considering the nonlinear shear behaviour of the 0°/90° interface. Finally, the question why two different second damage modes might occur in a laminate with similar geometry is considered.

2. Experiments

2.1. Test procedure

A cross-ply laminate, $[0/90_4]_s$, with a thick middle 90° layer has been made out of Hexcel IM7/8552 pre-impregnated carbon fibre sheets. Cross-ply glass/epoxy end-tabs 2.5 mm thick

were bonded after curing and then the plate was carefully cut into fourteen 1.25×10×300 mm specimens using a diamond wheel saw.

To examine the damage progress, different load levels were selected for each of the specimens. One of the specimens was loaded up to final failure which is due to fibre failure of the 0° layers. The load levels of the other specimens were selected accordingly to cover the different stages of damage development. The specimens were then loaded in displacement control at a rate of about 0.2mm/min up to their predefined load level. At this point, loading was stopped and the specimens were unloaded. An Instron extensometer with 50mm gauge length was used for strain measurements.

The edges of the specimens after testing were then polished in different stages after removing the end-tabs. The removed material due to polishing was roughly 1 mm in the width direction. Then a ZEISS Axio Imager 2 microscope was used to view the edge of the samples. To obtain the crack pattern over the length of the specimen, individual photos taken from the edge of the specimens were stitched together with the Axio Vision software. Crack measurements were also performed on the overall stitched image of the specimen using the same software. To quantify the damage pattern, the distance of all of the transverse cracks were measured at the mid-plane of the specimens. For a limited number of specimens, the variation of crack pattern through the width of the specimen was investigated by re-grinding and re-polishing the edge of the specimens in two separate stages by removing about 3 mm from the edge of the specimens and it was found that the damage pattern stayed approximately constant in the width direction.

2.2. Test results-Transverse cracking

A summary of the measured transverse cracking distances in the different specimens in addition to the maximum stress and strain are shown in Table 1. Figure 2 indicates the maximum stress and strain in different specimens in addition to the stress-strain curve of specimen no. 14 with

the largest applied load. Specimen no. 1 was not loaded but was polished and then viewed via the microscope to make sure that there were not any unpredicted cracks in the specimens before load application due to the process of making the test samples e.g. curing and cutting. Specimen no. 14 was loaded up to final failure and because of fibre failure of the 0° layers, it was not examined via microscopy. The other specimens were carefully viewed and snapshots were taken of their edges. No damage was observed in specimens no. 2 and 3, while a few of randomly distributed straight transverse cracks started to be observed in specimen no. 4 at a maximum applied strain of 0.3%.

Figure 3 indicates the average, maximum and minimum measured distances between the transverse cracks in samples no. 2-13. In the initiation stage of the transverse cracking (low values of strains), the crack separations are higher and the difference between minimum and maximum distances are considerable. As the load is increased, the remaining space for new cracks becomes more restricted and the distance between transverse cracks decreases. The large difference between maximum and minimum crack spacing also decreases and they both tend to converge toward the average value. The difference between maximum, minimum and average value of distances between cracks can be used to judge how evenly the cracks are spread over the specimens. Figure 3 clearly shows that crack spacing in the early stages of crack initiation is significantly non-uniform but becomes more even at larger strains.

The crack density of each laminate was calculated independently by dividing the counted number of transverse cracks by the specimen length, and is depicted in Figure 4 for specimens no. 1-13. The density of transverse cracks increases with a decreasing rate up to the strain of 1.16% when final failure occurs.

The Coefficient of Variation (CV) of the crack spacing is shown in Figure 5. At low values of strain, it is large, but as the load increases, it decreases to about 40% which is still significant

and indicates a quite non-uniform distribution of transverse cracking even at high values of strain. However, this large CV remains almost constant at strains larger than 0.65%.

The crack pattern taken from the edge of specimens no 8, 9, 11 and 13 is shown in Figure 6. The crack density is obviously increasing with the applied load. Furthermore, all of the cracks in specimens no. 8 and 9 are straight and perpendicular to the loading direction, but in specimens 10 and 11 loaded to higher strains, tiny oblique cracks in addition to some curved transverse cracks can be distinguished. All of the specimens were carefully viewed but no delamination was observed. It seems that the damage mode changes from transverse cracking to oblique cracks at larger values of applied strain. The oblique cracks occurring close to a straight transverse crack have been selected for more experimental quantification as the second damage mode of the tested laminate.

2.3. Test results- Oblique cracks

In specimens no 11-13, several small cracks close to the straight transverse cracks were observed. These oblique cracks do not run through the whole thickness of the 90° layers and are not also perpendicular to the loading direction. One of their tips is on the 0°/90°interface while the other approaches the straight transverse crack at an angle of about 50°-60° and stops before joining it. Two instances of these oblique cracks in specimens no. 11 and 13 are shown in Figure 7. To examine any change of crack pattern in the width direction, a quarter of the width of specimen 13 was ground in two separate stages. The observed crack pattern including both straight and oblique cracks was found unchanged.

The distance between the ends of the oblique and transverse cracks on the 0/90 interface in specimen 13 in addition to the length and angle of the oblique cracks with the 0/90 interface have been measured as shown in Figure 8. The measured length of the oblique crack ends is plotted against the distance between the oblique and transverse crack tips in Figure 9 (a) and there is a clear correlation between them, with the oblique crack getting longer when they are

further from the transverse crack. On the other hand, Figure 9 (b) indicates that the angles of the oblique cracks are approximately constant and independent of their position. It is worth mentioning that the minimum distance between the tips of the oblique and transverse cracks is more than 200μm which will be addressed in the next section. The average and coefficient of variation of the oblique crack's length, angle and the distance to the transverse crack normal to the loading direction is shown in Table 2. The standard deviation of all three parameters is less than the minimum measured standard deviation of the transverse crack distance in Table 1. Furthermore, the variation of angle of the oblique cracks is less than 10%, showing its repeatability.

3. Analysis of oblique cracks

Two separate FE analyses of oblique cracking are performed in this section. In the first series, the stress distribution around the transverse crack with different assumptions is examined and in the second approach, the damage mode change with two different transverse crack densities is investigated. The IM7/8552 material properties used in both of the analyses are given in Table 3. In both series of the analyses, 2D plane strain quadratic elements have been used for the 0° and 90° layers. The applied plane strain condition may introduce some in-plane transverse stresses which are not important and should not have a significant effect on the other stress components.

A mixed-mode bilinear cohesive model based on [23] is applied for the interface elements unless it is explicitly mentioned. An in-house FE solver is applied for the all analyses and has been validated on different problems [24-26]. A -180 °C uniform temperature decrease has been applied before the mechanical loading to account for the residual thermal stresses. The penalty stiffness of the cohesive elements has been assumed to be 5×10^5 N/mm^{-3} which is a normal value for such an analysis[25].

3.1. Crack initiation

To investigate the reason for crack initiation, two different unit cell models with the same 2 mm length and transverse cracks in the 90° layers on each boundary have been analysed (Figure 10). The nodes on the left side of the 0° layers are constrained in the x direction and a uniform displacement is applied on the right hand side nodes of the 0° layers. Linear elastic material properties were assigned to one of the models while in the other, damageable bilinear cohesive elements [23] have been applied at the 0°/90° interface. The response of the model including nonlinearity due to interfacial damage can be assumed closer to reality. The normal and shear strengths of the cohesive elements have been set equal to 121MPa and 82MPa according to the Hexcel data sheet for neat 8552 resin and reference [27]. Other material properties were kept linear elastic.

Figure 11 indicates the variation of maximum principal stress (S_1) in the 90° layer adjacent to the 0°/90°interface, obtained from the linear elastic and nonlinear models at the same strain of 1.0%. The distribution of S_1 in the middle of the unit-cell and far away from the transverse cracks is almost the same in both models, however around the transverse cracks at x=0 mm and x=2 mm, they are completely different. In the elastic model, the value of S_1 increases severely due to the singularity of the stress at the crack tip but in the model with cohesive elements at the interface, it decreases gradually. The point with maximum S_1 in the elastic model is also very close to the straight transverse cracks but due to interlaminar damage at the interface of the model with nonlinear cohesive elements, it moves away towards the middle of the unit-cell. This clearly indicates that considering the interlaminar damage at the 0°/90° interface causes stress suppression around the straight crack tips and lowers the probability of oblique crack initiation just next to the transverse crack tip whereas for points at a distance of about 0.4mm away from the straight transverse cracks, oblique crack initiation is more likely to happen.

The distribution of S_1 at 0.7% strain clearly shows that both the value and position of the point with maximum S_1 are variable. Therefore, the oblique cracks cannot initiate until the value of S_1 at the interface become larger than the strength of the 90° layer there. The scatter in the observed position of oblique crack initiation can also be described by the scatter in the strength of the material around the interface.

The distribution of maximum principal stress (S_1) in the 90° layer obtained from the nonlinear model at 1.0% strain is shown in Figure 12. It is clear that the points around the interface at a distance of about 0.4mm from the crack are prone to damage initiation. On the enlargement of the left bottom quarter of the model, the probable crack directions due to opening mode based on the maximum principal tensile stress are also indicated. This suggests that if a crack initiates from the area with high values of S_1 in opening mode, the crack would propagate in an oblique manner towards the closer transverse crack, making an angle of about 60° with the interface. However, this stress distribution changes after crack initiation.

3.2. Crack propagation

To study the damage mode change, crack propagation in two different models with similar properties but different lengths of L=2mm and L=4mm as shown in Figure 13 are modelled. A row of cohesive element is placed in the middle between the two transverse cracks and another row has been placed in an inclined manner with a distance of d_{oc}=0.6mm from the right transverse crack to represent the alternative likely locations of the next cracks. The angle of the inclined cohesive element row at the 0°/90° interface is assumed to be 61.1° according to the experimental observation in Table 2. The material properties in Table 3 were used for the both models. The comparison of these results shows the effect of transverse crack density on the damage mode.

Transverse cracking and delamination are both dominated by matrix material properties. Therefore similar shear and tensile material properties along with a mixed-mode crack

propagation formulation [23] which can distinguish between different loading types is a reasonable assumption[28].

The contours of stress in the x direction (S_x) in the 90° layer obtained from the models are shown in Figure 14 and Figure 15. When the distance between the two transverse cracks is 4mm (Figure 14), damage grows at the cohesive elements at the middle of the unit-cell producing a straight transverse crack and therefore the density of transverse cracks increases. But in the other model with the length of L=2mm, the oblique crack opens before the normal transverse cracking occurs (Figure 15). The slight stress redistribution around the cohesive elements at the middle shows that the damage process has started here but since there was not enough driving force (energy release rate), the damage has not propagated in the middle of the specimen. Therefore, it can be concluded that the tendency for crack propagation as an oblique crack increases for a higher transverse crack density, which agrees well with the experimental observations.

3.3. Effect of mode-II toughness

To investigate the effect of toughness of the interface in mode II, the 2 mm model described in the previous section (Figure 13) was run again keeping all of the material properties as before except the value of G_{IIc} which was changed to 0.2, 0.4 and 0.6 N/mm in three different runs. The loading and boundary conditions of all of the models are exactly the same, so their initial status (before crack propagation in any of the cohesive elements) is just as shown in Figure 15. The contours of x direction stress just after activation of one of the potential cracks are shown in Figure 16. In the case of G_{IIc}=0.2 N/mm, delamination occurs from the tips of the left transverse crack at a strain of 0.76% and suddenly propagates to almost the middle of the unit-cell. The second damage mode is still delamination for G_{IIc}=0.4 N/mm but it happens at a larger strain of 0.97%. The catastrophically delaminated area in this case is less than in the previous model with G_{IIc}=0.2 N/mm. Increasing the value of G_{IIc} to 0.6 N/mm changes the secondary

damage mode to an oblique crack at 0.91% strain. Therefore, it is clear that for lower values of G_{IIc}, delamination is the main second damage mode but as the shear toughness of the material is increased, the damage mode changes to oblique cracking.

Such a conclusion is intuitive since delamination occurs just due to shear loading and oblique cracks happen in tension. So if the shear toughness of the material is increased while the opening toughness is kept constant, cracks due to tension are more likely to take place. When the mode I toughness is kept constant in different models and the mode II toughness is increased, the resisting force against mode II loading is increased and therefore, damage modes due to mode I loading i.e. oblique cracks are more likely to occur.

This can explain why delamination has been reported in the literature as the secondary damage mode for the same $[0/90_4]_s$ layup and similar configuration in [3, 4]. The toughness of the applied material in [3, 4] is in a lower range (between 0.3 and 0.6 N/mm) and accordingly, delamination was reported as the secondary damage mode. However, the shear toughness of the material used in the present study is G_{IIc}=1.0 N/mm which is significantly higher, and shows why the secondary damage mode in these two studies are different.

The difference between the opening and shear toughness can reflect the possibility of oblique cracking. In the cases where the G_{IIc} is closer to G_{Ic}, delamination is favoured, but when G_{IIc} is considerably larger than G_{Ic}, oblique cracking is more prone to occur. In this specific study with the particular material and layup, if the mode I toughness is more than half of the mode II toughness, delamination induced by transverse cracking is the second damage mode of the laminate. More generally, in cross-ply laminates with newer toughened materials where the value of G_{IIc} is much higher than G_{Ic}, oblique cracks are more likely.

4. Conclusion

The damage growth of a $[0/90_4]_s$ cross-ply laminate has been investigated experimentally and numerically in this paper. Different loads have been applied to 14 tensile specimens and their

damage pattern has been observed by microscopy from the edge after surface preparation. The distance between the transverse cracks was measured on the stitched photos of the edges of each of the specimens.

The results clearly indicate the random nature of transverse cracks, especially in the starting phase. The minimum observed coefficient of variation of the distance between transverse cracks over the entire loading range was 40% which clearly indicates the variability of this damage mode. At high values of crack density, oblique cracks close to the transverse cracks were observed. No delamination induced by transverse cracking was detected in any of the specimens.

In the analyses of the oblique cracks, it was found that by considering damageable cohesive elements, the point with the highest value of maximum principal stress (S_1) moves away from the tips of the transverse cracks. Therefore, oblique cracks cannot initiate within approximately 0.25 mm of the normal transverse cracks. The experimentally observed path of the oblique cracks was also perpendicular to the plane with the maximum tensile stress which supports the idea of mode I crack propagation as the dominant damage mode.

The effect of transverse crack density on the damage mode was also studied with the FE simulations using two different representative volume elements with different lengths. The results showed that in the longer model, the first damage mode was transverse cracking but in the shorter one, an oblique crack occurred first. This result is also in agreement with the change in damage mode with increasing transverse-crack density, as observed in the experiments.

In the last part of the analysis, the effect of mode II toughness was studied on the damage mode. In cases with lower mode II toughness, delamination initiating from the tips of the transverse cracks was the secondary damage mode but in models with higher mode II toughness, oblique cracks occurred. This comparison can explain why different secondary damage modes have

been found for the same layup. It seems that with the newer toughened resin systems with higher mode II toughness, delamination induced by transverse cracking is less likely to happen.

5. References

[1] Katerelos DG, McCartney LN, Galiotis C. Local strain re-distribution and stiffness degradation in cross-ply polymer composites under tension. Acta Materialia. 2005;53(12):3335-43.
[2] O'Brien TK. Analysis of Local Delamination and their Influence on Composite Laminate Behavior. In: Johnson WS, editor. Delamination and Debonding of Materials, ASTM STP 876: American Society for Testing and Materials; 1985. p. 282–97.
[3] Takeda N, Ogihara S. Initiation and growth of delamination from the tips of transverse cracks in CFRP cross-ply laminates. Composites Science and Technology. 1994;52(3):309-18.
[4] Takeda N, Ogihara S. In situ observation and probabilistic prediction of microscopic failure processes in CFRP cross-ply laminates. Composites Science and Technology. 1994;52(2):183-95.
[5] Berthelot JM, Le Corre JF. A model for transverse cracking and delamination in cross-ply laminates. Composites Science and Technology. 2000;60(7):1055-66.
[6] Dharani LR, Wei J, Ji FS, Zhao JH. Saturation of Transverse Cracking with Delamination in Polymer Cross-Ply Composite Laminates. International Journal of Damage Mechanics. 2003;12(2):89-114.
[7] Hashin Z. Analysis of cracked laminates: a variational approach. Mechanics of Materials. 1985;4(2):121-36.
[8] Kashtalyan M, Soutis C. Analysis of matrix crack-induced delamination in composite laminates under static and fatigue loading. In: Harris B, editor. Fatigue in Composites: Woodhead Publishing and CRC Press; 2003.
[9] Lim S-H, Li S. Energy release rates for transverse cracking and delaminations induced by transverse cracks in laminated composites. Composites Part A: Applied Science and Manufacturing. 2005;36(11):1467-76.
[10] McCartney LN. PREDICTING TRANSVERSE CRACK FORMATION IN CROSS-PLY LAMINATES. Composites Science and Technology. 1998;58(7):1069-81.
[11] Nairn JA. The strain energy release rate of composite microcracking: a variational approach. Journal of Composite Materials. 1989;23:1106-29.
[12] Nairn JA, Hu S. The Initiation and Growth of Delamination Induced by Matrix Microcracks in laminated Composites. International Journal of Fracture. 1992;57:1-24.
[13] Ogihara S, Takeda N. Interaction between transverse cracks and delamination during damage progress in CFRP cross-ply laminates. Composites Science and Technology. 1995;54(4):395-404.
[14] Rebière JL, Maâtallah MN, Gamby D. Initiation and growth of transverse and longitudinal cracks in composite cross-ply laminates. Composite Structures. 2001;53(2):173-87.
[15] Farrokhabadi A, Hosseini-Toudeshky H, Mohammadi B. A generalized micromechanical approach for the analysis of transverse crack and induced delamination in composite laminates. Composite Structures. 2011;93(2):443-55.
[16] Hu S, Bark JS, Nairn JA. On the phenomenon of curved microcracks in [(S)/90n]s laminates: Their shapes, initiation angles and locations. Composites Science and Technology. 1993;47(4):321-9.
[17] Boniface L, Smith PA, Bader, M. G., Rezaifard AH. Transverse Ply Cracking in Cross-Ply CFRP Laminates--Initiation or Propagation Controlled? Journal of Composite Materials. 1997;31(11):1080-112.
[18] Groves SE, Harris CE, Highsmith AL, Allen DH, Norvell RG. An experimental and analytical treatment of matrix cracking in cross-ply laminates. Experimental Mechanics. 1987;27(1):73-9.
[19] Salpekar SA, O'Brien TK. Combined Effect of Matrix Cracking and Stress-Free Edge on Delamination. NASA; 1990.
[20] Wang ASD, Kishore NN, Li CA. Crack development in graphite-epoxy cross-ply laminates under uniaxiat tension. Composites Science and Technology. 1985;24:1-31.

[21] Jalalvand M, Hosseini-Toudeshky H, Mohammadi B. Numerical modeling of diffuse transverse cracks and induced delamination using cohesive elements. Proceedings of the Institution of Mechanical Engineers, Part C: Journal of Mechanical Engineering Science. 2012.
[22] Okabe T, Nishikawa M, Takeda N. Numerical modeling of progressive damage in fiber reinforced plastic cross-ply laminates. Composites Science and Technology. 2008;68(10–11):2282-9.
[23] Camanho PP, Davila CG, de Moura MF. Numerical Simulation of Mixed-Mode Progressive Delamination in Composite Materials. Journal of Composite Materials. 2003;37(16):1415-38.
[24] Jalalvand M, Hosseini-Toudeshky H, Mohammadi B. Numerical modeling of diffuse transverse cracks and induced delamination using cohesive elements. Proceedings of the Institution of Mechanical Engineers, Part C: Journal of Mechanical Engineering Science. 2012;227(7):1392-405.
[25] Jalalvand M, Hosseini-Toudeshky H, Mohammadi B. Homogenization of diffuse delamination in composite laminates. Composite Structures. 2013;100(0):113-20.
[26] Jalalvand M, Czél G, Wisnom MR. Numerical modelling of the damage modes in UD thin carbon/glass hybrid laminates. Composites Science and Technology. 2014(0).
[27] May M, Hallett SR. An assessment of through-thickness shear tests for initiation of fatigue failure. Composites Part A: Applied Science and Manufacturing. 2010;41(11):1570-8.
[28] Canturri C, Greenhalgh ES, Pinho ST, Ankersen J. Delamination growth directionality and the subsequent migration processes – The key to damage tolerant design. Composites Part A: Applied Science and Manufacturing. 2013;54(0):79-87.
[29] Huang C-Y, Trask RS, Bond IP. Characterization and analysis of carbon fibre-reinforced polymer composite laminates with embedded circular vasculature. Journal of The Royal Society Interface. 2010;7(49):1229-41.
[30] Hallett SR, Green BG, Jiang WG, Wisnom MR. An experimental and numerical investigation into the damage mechanisms in notched composites. Composites Part A: Applied Science and Manufacturing. 2009;40(5):613-24.

Table 1- Maximum stress and strain of different samples in addition to the summary of the measured distances between transverse cracking

Specimen No.	Max. Stress (MPa)	Max. Strain (%)	Average crack spacing (mm)	Standard deviation (mm)	CV (%)	crack density (1/mm)	Min. crack spacing (mm)	Max. crack spacing (mm)
1	0	0	--	--	--	0	--	--
2	82.9	0.2	--	--	--	0	--	--
3	106.4	0.25	--	--	--	0	--	--
4	115.9	0.3	19.53	28.17	144%	0.05	3.09	69.41
5	146.6	0.35	17.37	16.42	94%	0.06	3.14	42.33
6	159	0.4	9.67	13.88	143%	0.1	2.03	45.70
7	184.1	0.45	4.30	2.85	66%	0.23	1.72	12.25
8	212.4	0.55	3.60	2.23	61%	0.28	1.33	17.35
9	258.5	0.65	2.23	0.91	40%	0.45	0.74	4.24
10	340.4	0.86	1.60	0.64	40%	0.62	0.39	2.83

11	383.5	0.97	1.37	0.56	41%	0.73	0.28	2.49
12	424	1.16	1.21	0.49	40%	0.83	0.29	2.25
13	430.5	1.13	1.19	0.51	42%	0.84	0.32	2.51
14	464.9	1.24	--	--	--	--	--	--

Table 2- Average and standard deviation of length, angle and distance of oblique cracks tip from the tips of main transverse crack (see Figure 8 and 13)

	Distance of oblique and straight transverse crack tips, d_{oc} (μm)	**Length (μm)**	**Angle, θ (deg)**
Average	409	400	61.1
Standard Deviation	84	118	5.8
CV (%)	20.5%	29.5%	9.6%

Table 3-IM7/8552 material properties [29, 30]

E_1 (GPa)	E_2 (GPa)	G_{12} (GPa)	G_{23} (GPa)	ν_{12}	ν_{23}	α_{11} (K^{-1})	α_{22} (K^{-1})	G_{Ic} (N/mm)	G_{IIc} (N/mm)	Ply thickness (mm)
161.00	11.4	5.17	3.98	0.32	0.44	0.6×10^{-6}	28.6×10^{-6}	0.2	1.0	0.125

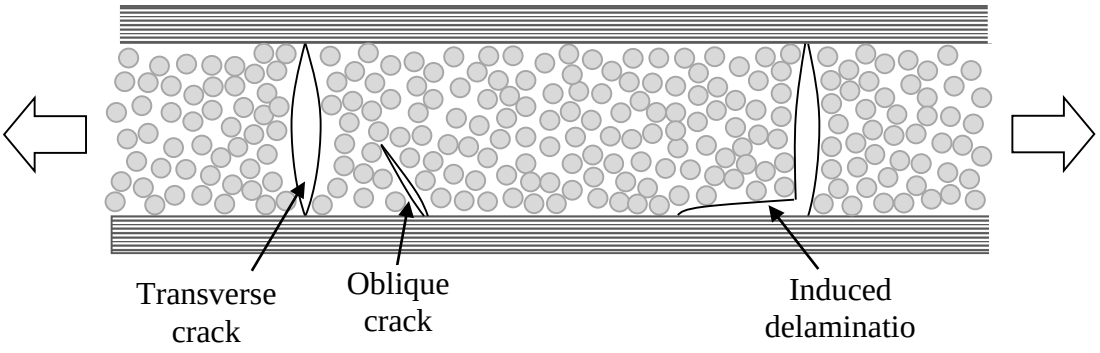

Figure 1- Different damage modes in a cross-ply laminates

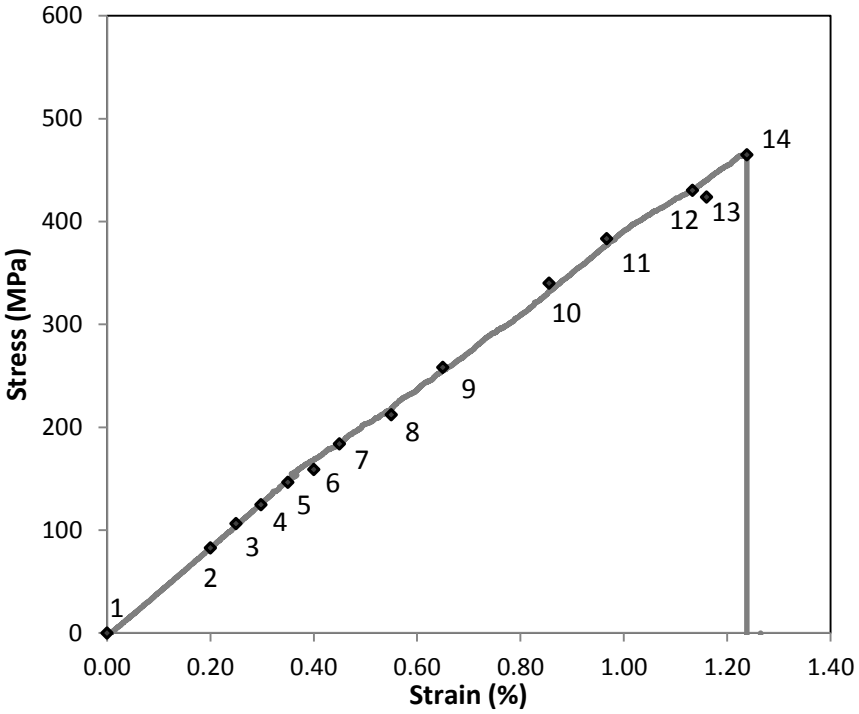

Figure 2-Stress-strain curve of specimen number 14 and maximum stress and strain of other interrupted test specimens

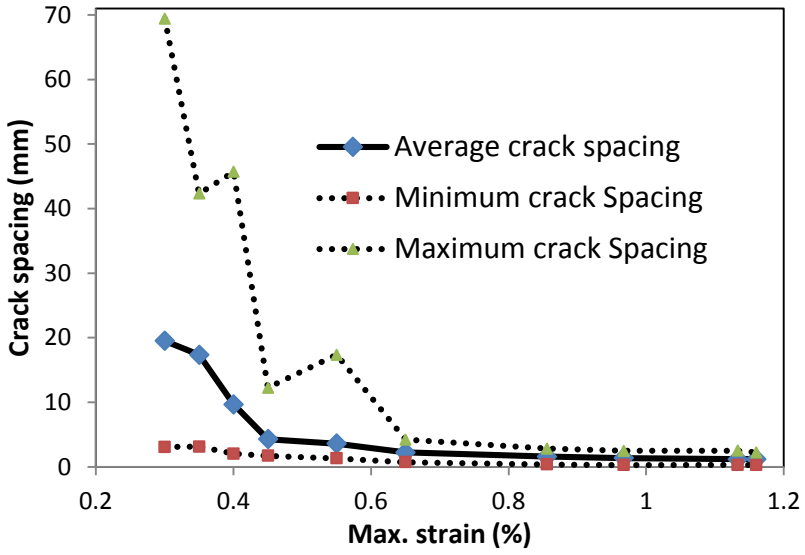

Figure 3-Average, maximum and minimum crack spacing of the specimens no. 4-13

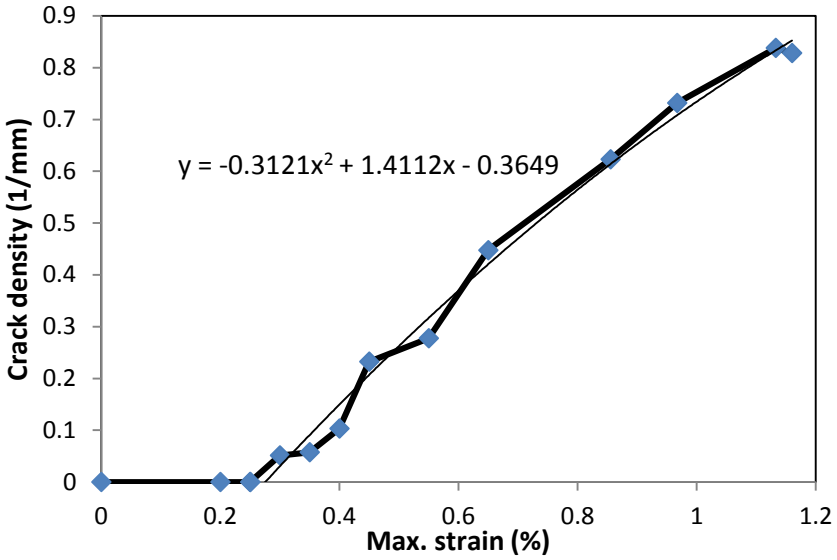

Figure 4- Crack density of specimens no. 2-13

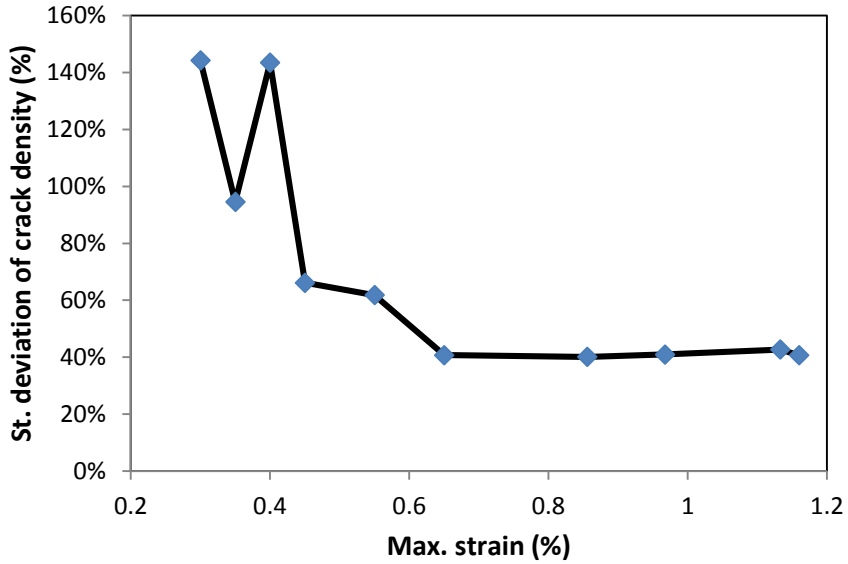

Figure 5- Coefficient of variation of transverse crack spacing of specimens no. 4-13

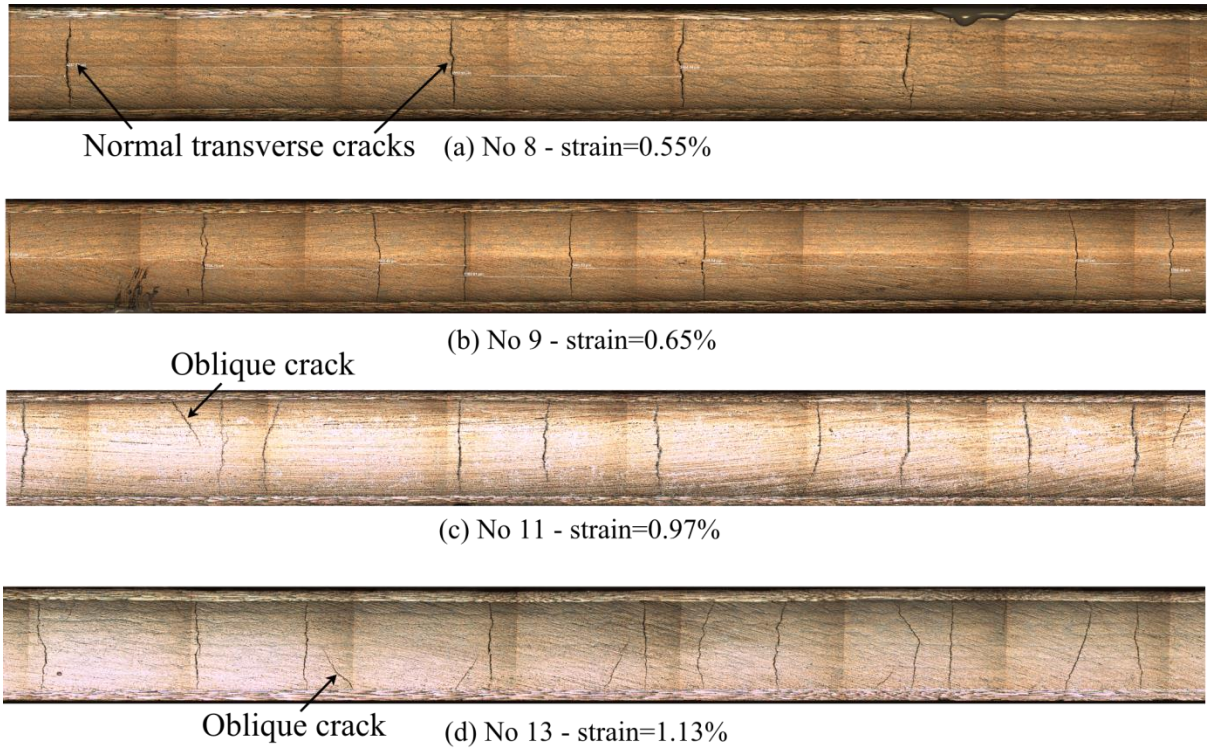

Figure 6- Edge view of a part of samples no. 8, 9, 11 and 13

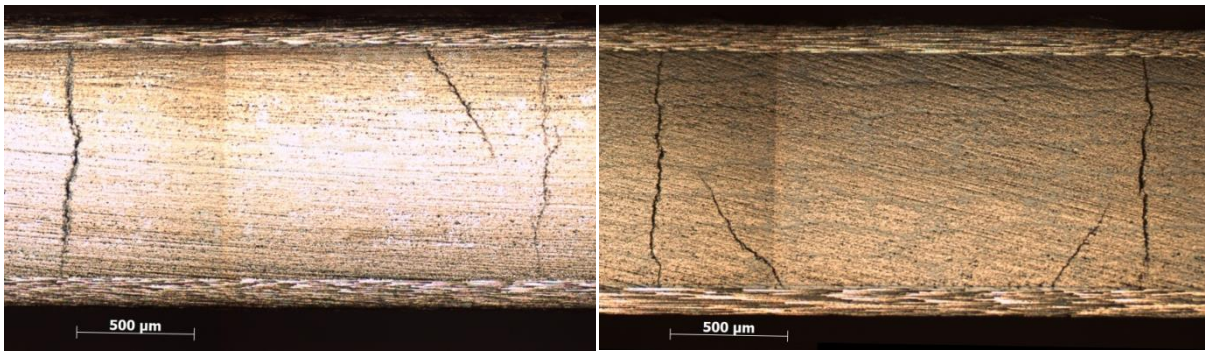

11 13

Figure 7- Oblique cracks in specimens no. 11 and 13

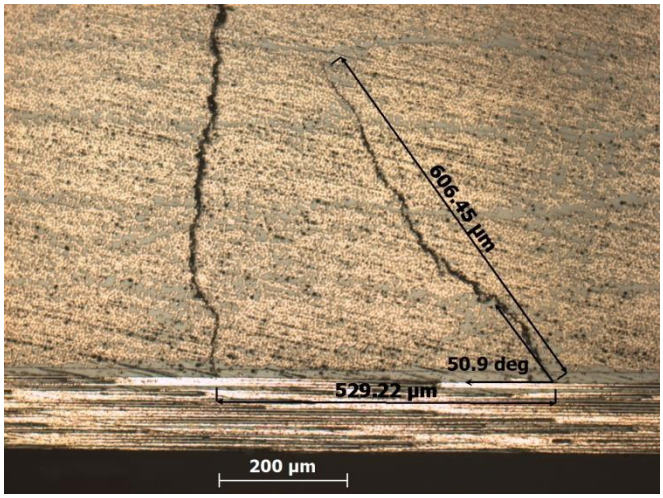

Figure 8- Measuring the distance between the oblique and straight transverse crack tips, oblique crack length and the angle between 0/90 interface and oblique crack

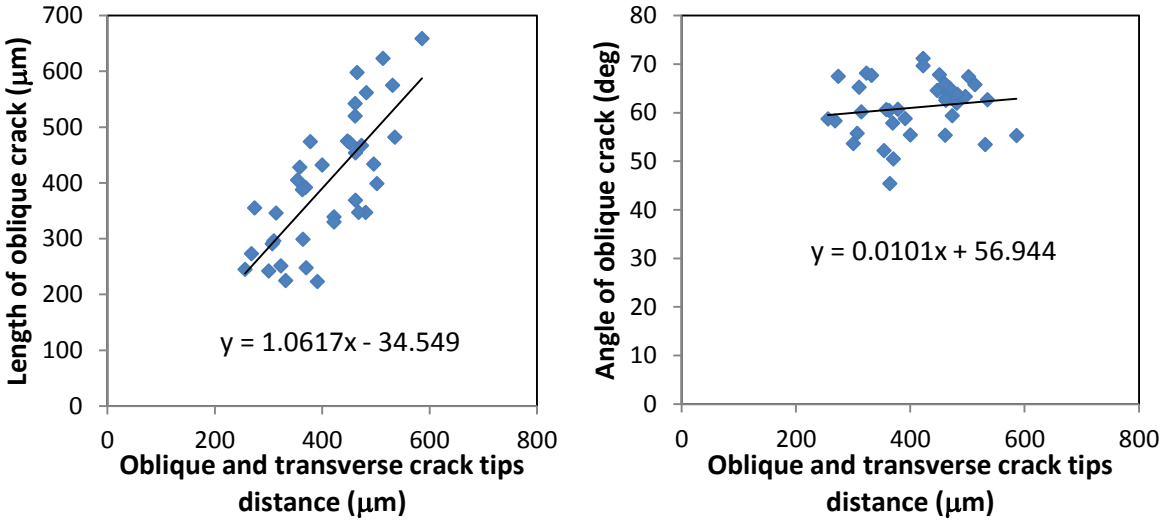

(a) (b)

Figure 9- (a) length and (b) angle of oblique crack tips measured in specimen no. 13

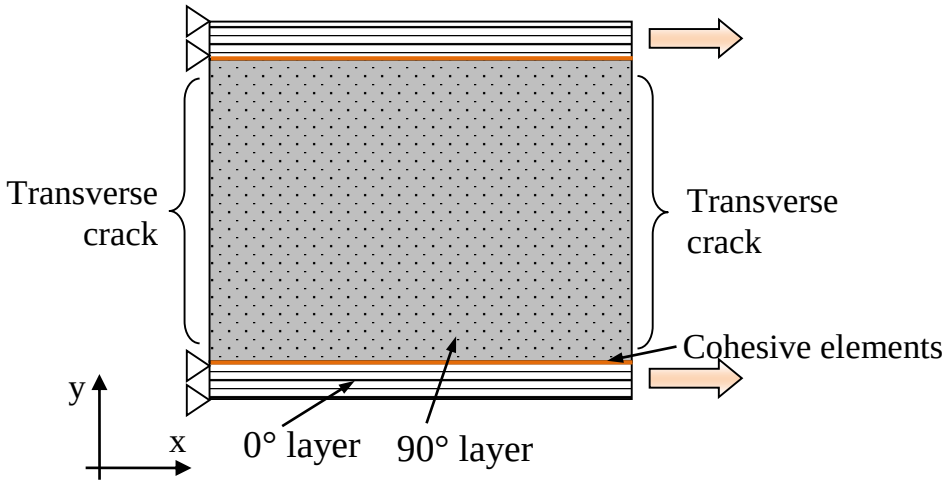

Figure 10- Unit-cell model for investigating oblique crack initiation

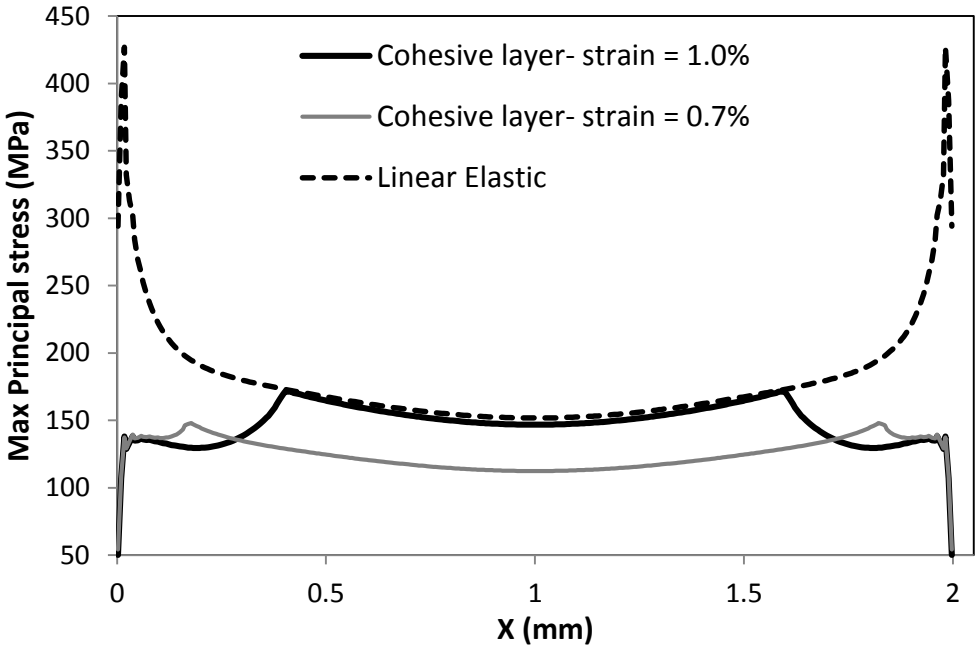

Figure 11- Maximum principal stress (S_1) at the 0°/90° interface

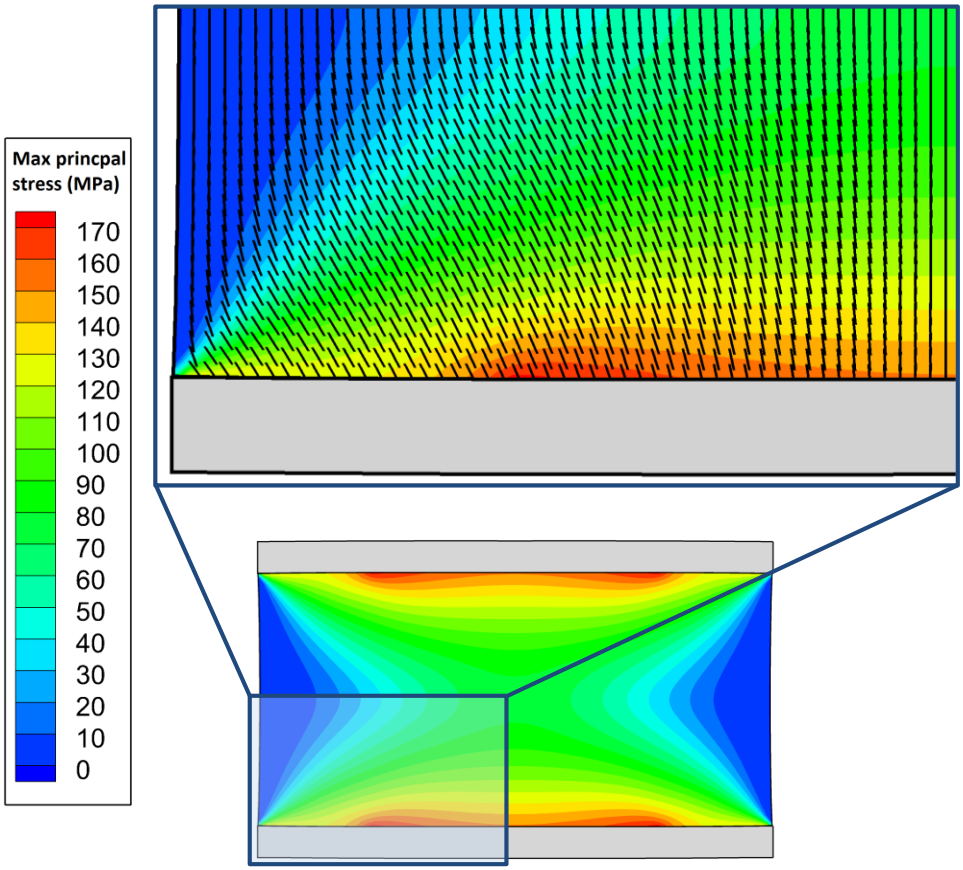

Figure 12- Contour of max principal stress (S_1) in 90° layer and the potential direction for crack initiation in a 2mm long unit-cell

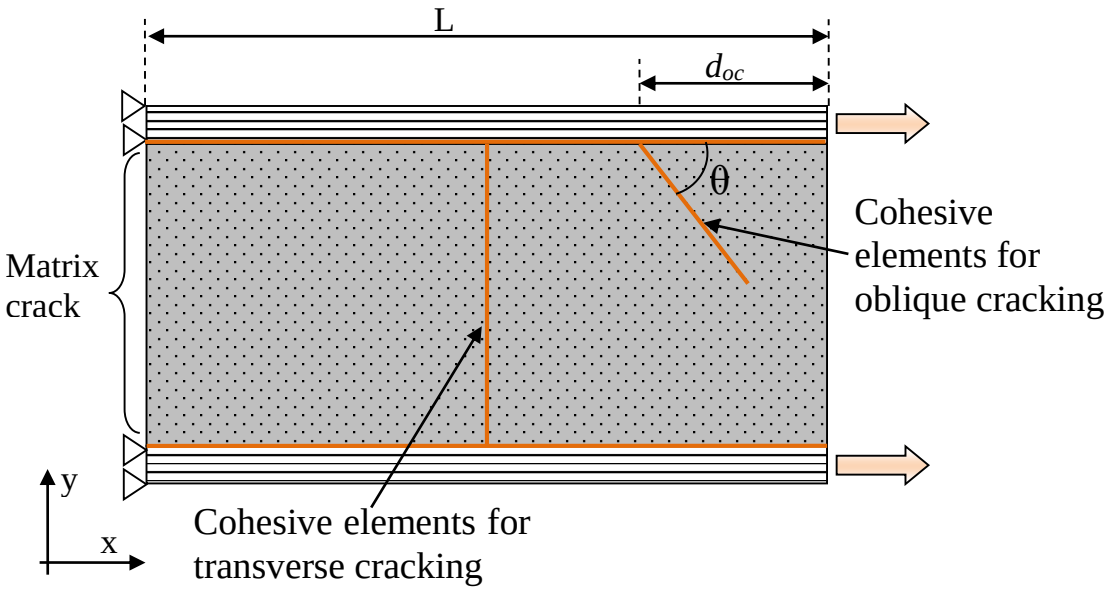

Figure 13- Unit-cell with cohesive elements at the middle and probable path of oblique crack

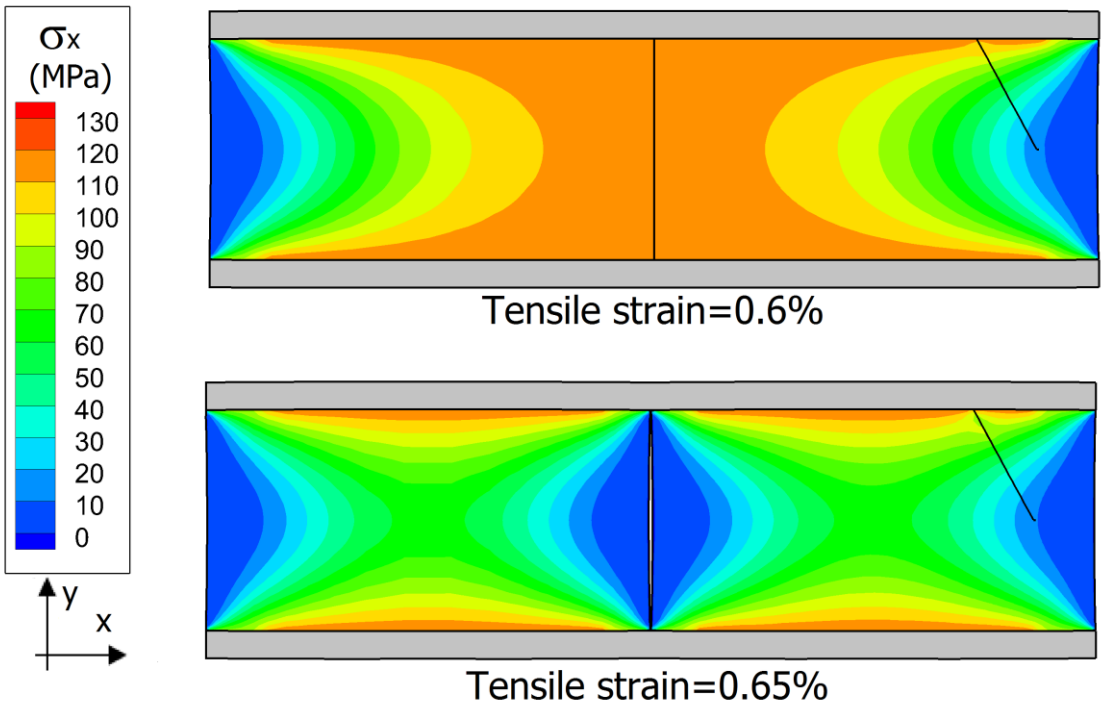

Figure 14- Transverse cracking in the unit-cell with length L=4mm

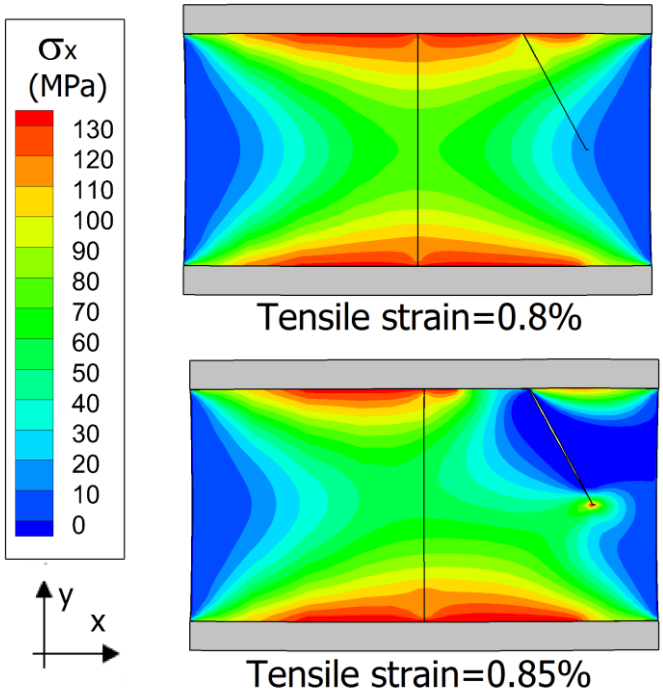

Figure 15- Oblique crack opening in the unit-cell with length L=2mm

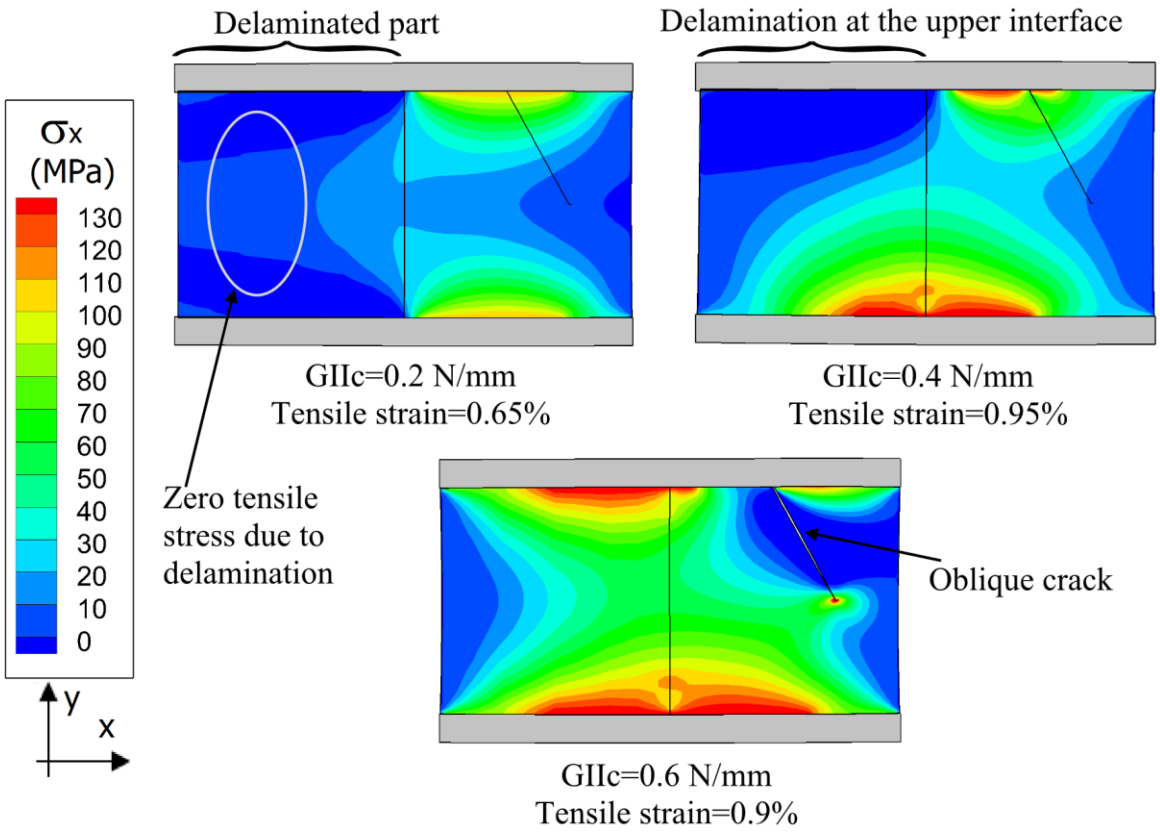

Figure 16- Effect of G_{IIc} on the secondary damage mode of the cross-ply laminates with similar G_{IC}=0.2N/mm